temperature-dependent measurements of the hyperfine constant A.

ACKNOWLEDGMENTS

The author expresses his appreciation to Dr. H. R. Lewis for his advice and encouragement during the course of this work. I am indebted to Dr. C. H. Anderson, Dr. Z. J. Kiss, Dr. S. R. Polo, and Dr. H. A. Weakliem for their many helpful discussions. The technical assistance of E. J. Kerdraon in designing some of the equipment and in taking the data is appreciated.

PHYSICAL REVIEW VOLUME 141, NUMBER 1 JANUARY 1966

Electrodynamic Study of Josephson Tunneling in Superconducting Junctions

A. H. SILVER, R. C. JAKLEVIC, AND J. LAMBE
Scientific Laboratory, Ford Motor Company, Dearborn, Michigan
(Received 9 August 1965)

We have performed a quantitative electrodynamic experiment on a Josephson oxide tunneling junction. Using a current source at 30 Mc/sec, we have verified the time dependence of the Josephson equation, $j=j_0 \sin[\gamma_l-\gamma_r-(2e/\hbar)\int \mathbf{A}\cdot\mathbf{dl}]$, where $(\partial/\partial t)[\gamma_l-\gamma_r-(2e/\hbar)\int_l^r \mathbf{A}\cdot\mathbf{dl}]=-(2eV/\hbar)$. Thus the limiting voltage is shown to obey the quantum relationship, $2eV=\hbar\omega$. Measurements were made completely in the coherent state showing the diffraction nature of the junction as a function of applied magnetic field. The Josephson (parametric) inductance of the junction was directly observed and is in good agreement with the theory.

INTRODUCTION

JOSEPHSON[1] first predicted that a sufficiently thin tunneling junction between two superconductors would support a lossless tunneling current. He concluded that the current would be dc at zero voltage difference but that an alternating supercurrent would flow at finite voltages. Anderson[2] and Josephson[3] extended and interpreted the initial prediction in terms of the quantum phase difference of the superconducting order parameter or wave function at the two sides of the junction.

Experimental verification of the dc Josephson effect has been provided by a number of separate experiments[4–7] which elucidated the stationary quantum-wave interference properties of superconducting circuits containing one or more Josephson junctions. The Josephson ac effect has been observed via detection in the junction itself by Shapiro[8] and others.[9,10] While the one approach of attempting to generate ac with the application of a dc voltage across the junction was under way in several laboratories, we chose to investigate the Josephson ac effect dynamically by a different experimental approach, namely, to observe the dynamic characteristics of a Josephson junction under the influence of a radio-frequency current source. This investigation is reported here with quantitative measurements of the quantum voltage, the Josephson inductance, and the superconducting phase difference in the coherent state averaged over the surface of the junction.

THEORY

The fundamental equations relating to the Josephson effect express the phase-dependent part of the binding or coherence energy per unit area and the supercurrent density for weakly coupled superconductors as

$$E(\mathbf{r},t)=E_0\cos\left[\gamma_l-\gamma_r-\frac{2e}{\hbar}\int_l^r \mathbf{A}\cdot\mathbf{dl}\right], \quad (1)$$

and

$$j(\mathbf{r},t)=j_0\sin\left[\gamma_l-\gamma_r-\frac{2e}{\hbar}\int_l^r \mathbf{A}\cdot\mathbf{dl}\right], \quad (2)$$

where $[\gamma_l-\gamma_r-(2e/\hbar)\int_l^r A\cdot dl]$ is the gauge-invariant phase difference across the junction. We will explicitly concern ourselves with oxide junctions and use the coordinate definitions of Fig. 1. The phase difference $[\gamma_l-\gamma_r-(2e/\hbar)\int_l^r \mathbf{A}\cdot\mathbf{dl}]$ will be a function of $(\mathbf{r},t)$

[1] B. D. Josephson, Phys. Letters **1**, 251 (1962).
[2] P. W. Anderson, *Lectures on the Many Body Problem*, edited by E. R. Caianiello (Academic Press Inc., New York, 1964), Vol. 2, p. 113.
[3] B. D. Josephson, Rev. Mod. Phys. **36**, 216 (1964).
[4] P. W. Anderson and J. M. Rowell, Phys. Rev. Letters **10**, 230 (1963).
[5] J. M. Rowell, Phys. Rev. Letters **11**, 200 (1963).
[6] M. D. Fiske, Rev. Mod. Phys. **36**, 221 (1963).
[7] R. C. Jaklevic, J. Lambe, A. H. Silver, and J. E. Mercereau, Phys. Rev. Letters **12**, 159 (1964); Phys. Rev. Letters **12**, 274 (1964); *Proceedings of the Ninth International Conference on Low Temperature Physics* (to be published); R. C. Jaklevic, J. Lambe, J. E. Mercereau, and A. H. Silver, Phys. Rev. **140**, A1628 (1965).
[8] S. Shapiro, Phys. Rev. Letters **11**, 80 (1963); S. Shapiro, A. R. Janus, S. Holly, Rev. Mod. Phys. **36**, 223 (1964).
[9] R. E. Eck, D. J. Scalapino, and B. N. Taylor, Phys. Rev. Letters **13**, 15 (1964).
[10] D. D. Coon and M. D. Fiske, Phys. Rev. **138**, A744 (1965).

such that

$$\frac{\partial}{\partial x}\left[\gamma_l-\gamma_r-\frac{2e}{\hbar}\int_l^r \mathbf{A}\cdot\mathbf{dl}\right]=\frac{2eBd}{\hbar}, \tag{3}$$

and

$$\frac{\partial}{\partial t}\left[\gamma_l-\gamma_r-\frac{2e}{\hbar}\int_l^r \mathbf{A}\cdot\mathbf{dl}\right]=-\frac{2eV}{\hbar}, \tag{4}$$

where $\mathbf{d}$ is twice the penetration length plus the thickness of the oxide.[3] The spatial dependence of $[\gamma_l-\gamma_r-(2e/\hbar)\int_l^r \mathbf{A}\cdot\mathbf{dl}]$ gives rise to the "diffraction"[3,5] and "interference"[7] effects demonstrated previously. The time-dependent term, Eq. (4), was invoked to explain the step voltage patterns of Shapiro.[8] A simultaneous solution of Eqs. (3) and (4) predicts standing electromagnetic waves in the junction and was investigated by Eck, Scalapino, and Taylor[9] and Coon and Fiske.[10]

Our interest is primarily in the time-dependent phase. We can separate the two phase contributions and then integrate over the area of the junction, the xz plane, with the resulting equation

$$I=I_0\sin\left[\frac{-2e}{\hbar}\int Vdt\right], \tag{5}$$

where

$$I_0=(j_0\sigma\hbar/e\Phi)\sin(e\Phi/\hbar), \tag{6}$$

and σ is the area of the junction. We will consider I_0 to be the maximum supercurrent which the junction will pass and we see by Eq. (6) that this value can be altered by the flux Φ in the manner used to produce the diffraction pattern.[5] Josephson[1,3] noted that if a voltage V existed, there would be an alternating supercurrent $I=I_0\sin\omega t$ where $\omega=2eV/\hbar$. We note that the Josephson equation is also satisfied for a symmetric square-wave voltage with a repetition rate or frequency given by $\nu=2eV/\hbar$.

Let us adopt the approach of a current source so that

$$I=I_s\sin\omega_s t, \tag{7}$$

where I_s and ω_s are the independent variables. If we equate the currents in Eqs. (5) and (7), we have

$$I_0\sin\left[\frac{-2e}{\hbar}\int Vdt\right]=I_s\sin\omega_s t, \tag{8}$$

where $\int Vdt$ will be real for $I_0\geq I_s$. Solving for V,

$$(-2eV/\hbar)=d/dt\{\text{arc sin}[(I_s/I_0)\sin(\omega_s t)]\}, \tag{9}$$

and

$$(-2eV/\hbar\omega_s)=(I_s/I_0)\cos(\omega_s t)\times[1-(I_s/I_0)^2\sin^2(\omega_s t)]^{-1/2}. \tag{10}$$

We can expect to represent V as a Fourier series in ω_s,

$$-2eV/\hbar\omega_s=\sum_{n=1}^{\infty} a_n\cos(n\omega_s t) \tag{11}$$

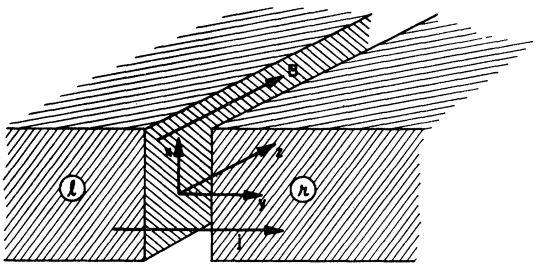

FIG. 1. Diagram of Josephson tunneling junction showing direction of current and magnetic field.

for which the amplitude of the fundamental is

$$a_1=\pi^{-1}\int_{-\pi}^{\pi}\frac{2eV}{\hbar\omega_s}\cos(\omega_s t)d(\omega_s t)$$

and from Eq. (10),

$$a_1=\pi^{-1}\frac{I_s}{I_0}\int_{-\pi}^{\pi}\cos^2(\omega_s t)\times\left[1-\left(\frac{I_s}{I_0}\right)^2\sin^2(\omega_s t)\right]^{-1/2}d(\omega_s t). \tag{12}$$

Since the integrand is an even function we can write this in the form of a complete elliptic integral[11]

$$a_1=\frac{4k}{\pi}\int_0^{\pi/2}\cos^2\varphi[1-k^2\sin^2\varphi]^{-1/2}d\varphi, \tag{13}$$

where $k=(I_s/I_0)$ and $\varphi=\omega_s t$.

Asymptotic solutions are given for $k^2\ll 1$ and for $(1-k^2)\ll 1$ as[11]

$$a_1=k[1+(k^2/8)+3(k^2/8)^2+\cdots], \quad k^2\ll 1, \tag{14}$$

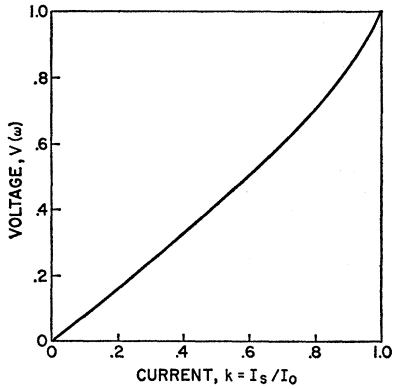

FIG. 2. Graph of the predicted rf voltage amplitude as a function of the rf current. The voltage amplitude is normalized to $(4/\pi)(\hbar\omega/2e)=(2\hbar\omega/\pi e)$ and the current is given as the fraction k of the maximum supercurrent, I_0.

[11] E. Jahnke and F. Emde, *Tables of Functions* (Dover Publications, Inc., New York, 1945), p. 73.

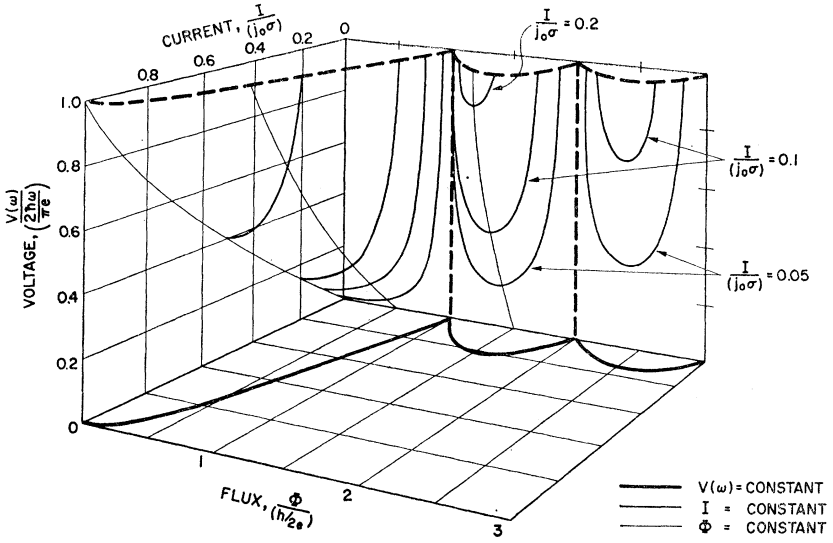

FIG. 3. Three-dimensional plot of the predicted rf voltage, $V(\omega)$, as a function of the supercurrent, k, and magnetic flux, Φ. The contour lines are in the k=constant and Φ=constant planes as indicated.

and

$$a_1=(4k/\pi)[1-(1/2)(\Lambda-3/2)(1-k^2) -(9/16)(\Lambda-17/12)(1-k^2)^2-\cdots], \quad (1-k^2)\ll 1, \quad (15)$$

where $\Lambda=\ln[4/(1-k^2)^{1/2}]$. The first harmonic of the voltage from Eq. (11) is

$$V(\omega_s)=-(\hbar\omega_s/2e)a_1\cos(\omega_s t), \quad (16)$$

where a_1 can be evaluated from tables of Eq. (13), or in asymptotic form from Eqs. (14) and (15). Figure 2 is a graph of Eq. (16) as a function of (I_s/I_0). The voltage at ω_s increases as $(\hbar\omega_s/2e)(I_s/I_0)$ near $I_s=0$ and varies as $(4/\pi)(\hbar\omega_s/2e)(I_s/I_0)$, as I_s approaches I_0. When $I_s=I_0$, the solution is the fundamental of a square wave whose amplitude is $(\hbar\omega_s/2e)$. We term this the quantum voltage.

Although this method of solution provides a continuous variation of the form and amplitude of V as (I_s/I_0) varies from zero to unity, direct substitution of $I_s=I_0$ in Eq. (10) gives only the constant solution $2eV=\hbar\omega_s$. This is a consequence of the multivalued nature of the angles in Eqs. (8) and (9) which should result in a $\pm$ prefix in Eq. (10).

Figure 3 is a three-dimensional representation of the behavior of the Josephson junction in the coherent mode. The voltage and current at the frequency ω are plotted for all values of the flux, Φ. The flux is assumed to be time-independent and the current is the independent variable as in the calculation above. The region of validity is defined by the diffraction curve in the (I,Φ) plane. In terms of the scaling constant for V, $(\hbar\omega/2e)$, the response will lie along some curve in (Φ,I,V) space.

We also wish to consider the effective inductance of the Josephson junction. Equation (10) can be recast as

$$V=-(\hbar/2e)[1-I^2/I_0^2]^{-1/2}d(I/I_0)/dt, \quad (17)$$

where I is the current as given by Eq. (7). Here we can characterize a parametric inductance as

$$L=(\hbar/2eI_0)[1-I^2/I_0^2]^{-1/2} \quad (18)$$

which is a function of time. We can also discuss an effective inductance defined by

$$-V_1\cos(\omega_s t)=L_1\omega_s I_s\cos(\omega_s t) \quad (19)$$

which from Eq. (16) gives

$$L_1=(\hbar/2e)a_1/I_s. \quad (20)$$

With a_1 given by Eq. (13), we have

$$L_1=\frac{4}{\pi I_0}\frac{\hbar}{2e}\int_0^{\pi/2}\cos^2\varphi[1-k^2\sin^2\varphi]^{-1/2}d\varphi. \quad (21)$$

The total variation of this inductance as I_s is varied from zero to I_0 is from $(\hbar/2eI_0)$ to $(4/\pi)(\hbar/2eI_0)$, respectively. However, the range of L_1 as I_0 varies from $I_{0\max}$ to zero is from $(1/I_{0\max})(4/\pi)(\hbar/2e)$ to infinity, respectively. $I_{0\max}$ is the maximum value of I_0 in Eq. (6) and is equal to $j_0\sigma$.

EXPERIMENT

The experiments were performed with Josephson Sn-SnO-Sn junctions fabricated by previously described techniques[7] and evaporated on a quartz substrate. The area of the junctions was about 0.3 mm×0.3 mm. The evaporated leads were essentially narrow striplines in each direction to provide minimum inductance leads as shown in Fig. 4(a). The experiments were performed near $T=3.5$°K in order to keep the measuring currents small.

In order to perform the electrodynamic experiments in a quantitative fashion we chose to operate near 30 Mc/sec. Although larger voltages are to be expected at higher frequencies, quantitative determination of the amplitudes and phases of I and V is more difficult.

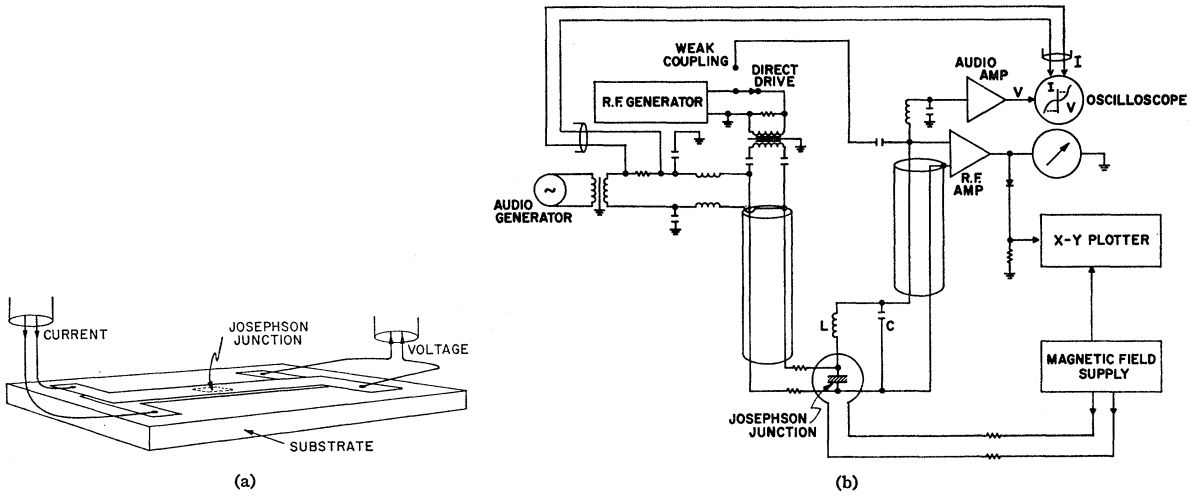

FIG. 4. (a) Experimental geometry of the Josephson junction and the measuring lead wires. (b) Block diagram of the electronic measuring system. The alternative methods of rf coupling to the junction are shown schematically by the switch labeled "direct drive" and "weak coupling."

Our experimental arrangement also provided for rapidly successive or simultaneous measurements of both the dc characteristics and rf properties of the junction without removing the sample from the liquid-helium bath. This scheme is shown in Fig. 4(b). A conventional four-point probe method with oscilloscope display of the low-frequency I-V characteristics was provided by the audiogenerator and audio amplifier. The rf response was accomplished with the same four-point leads and two twin-lead shielded cables. The LC circuit is used as a voltage and impedance step-up transformer with a voltage gain of Q at the resonance frequency. Proper decoupling of the rf and audio circuits was provided to maintain the Q of the rf resonant transformer.

The rf generator was connected as a current source. The characteristic impedance Z_0 of the resonant circuit was 10 Ω with the Q approximately 800. A Wallman-type cascade rf preamplifier was used with an over-all rf gain of 4000. The output voltage was measured with a Boonton Electronics Corp. Model 91-CA RF Voltmeter.

A magnetic-field-sweep unit provided variation of the flux in the junction and hence produced changes in I_0 as given in Eq. (6). The audiofrequency I-V characteristics were first observed for each junction. Only those junctions which showed the proper diffraction pattern of I_0 versus flux were considered to be Josephson junctions and were studied further. After a determination of $I_0(\Phi)$, the audiofrequency source was turned off and the flux set to zero. The rf current was turned on to a value I_s less than $I_{0\max}$ and the frequency ω_s of the rf generator tuned to the tank resonance. A background rf voltage appeared on the rf meter due to incidental coupling of the generating and receiving systems. As the magnetic field is varied the rf voltage level decreases to a minimum value when $I_0=I_s$. At this point $V(\omega_s)$ rises sharply. Furthermore the Q of the circuit is reduced by about 10^2 indicating that the junction is normal with a resistance about 1 Ω. As the flux increases I_0 decreases further to zero and then increases until $I_0=I_s$. At this point $V(\omega)$ returns to the same minimum value and the high Q of the circuit is restored.

A plot of this behavior of both I_0 and $V(\omega)$ as a function of Φ (as measured by the magnet current) for one Josephson junction is shown in Fig. 5. This data for $V(\omega)$ was taken with $I\simeq 10$ μA. Furthermore, notice that the magnitude of $V(\omega)$ at $I_0=I_s$ is the same for all observed positions. These data for I_0 and $V(\omega)$ represent the $V(\omega)=0$ and $I=10$ μA planes, respectively, of Fig. 3 can be compared with that theoretical graph.

The background rf voltage in Fig. 5 was about 200 mV (rms) at the rf meter and the over-all change upon varying the magnetic flux was 70 mV (rms). Referred to the first amplifier, the change in the voltage amplitude was then 25 μV. From Eq. (16) we expect the voltage change across the junction to be 7.3×10^{-8} V,

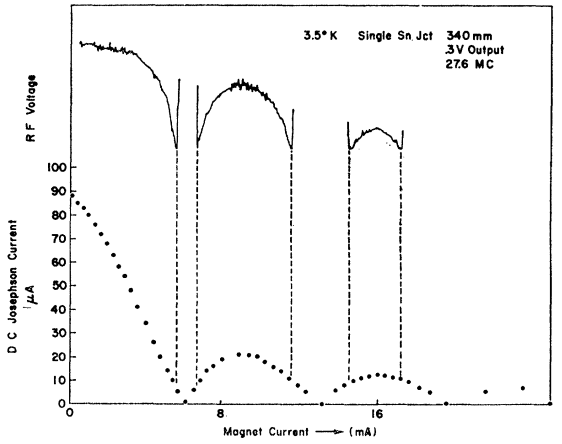

FIG. 5. Experimental data for I_0 and $V(\omega)$ as a function of the magnetic flux.

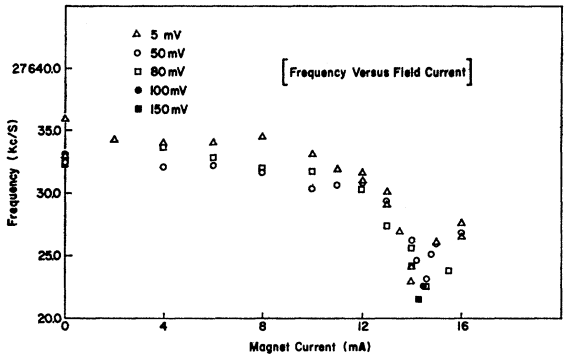

FIG. 6. Resonance frequency of LC circuit containing the junction as a function of magnetic field and rf supercurrent.

from which we would predict a voltage across the resonant circuit of $QV(\omega_s)=58.2\ \mu$V. However, we note from Eq. (21) that for $I_0=10\ \mu$A the inductive reactance of the junction at $I_s=I_0$ is $(V(\omega_s)/I_0)=7.3\times10^{-3}\ \Omega$, whereas the equivalent input resistance of the resonant circuit is $Z_0/Q=12.5\times10^{-3}\ \Omega$. When the entire circuit is considered at resonance, the dispersion voltage across the resonant circuit should be $0.44QV(\omega_s)$ compared to the measured voltage $0.43QV(\omega_s)$. The agreement is excellent.

A further demonstration of the nature of the ac Josephson effect is the direct observation of the parametric inductance. In Fig. 4(b) the rf source could be switched from direct connection to the Josephson junction to a loose coupling to the resonant circuit through a very small capacitor. Then the resonance frequency of the circuit can be measured as a function of I_0 and I_s by varying the magnetic flux and the voltage level, respectively. Figure 6 gives the variation of resonance frequency with magnetic field for a junction where the first null in $I_0(\Phi)$ occurs at 14.5 mA of magnet current. The ac supercurrent is measured by the ratio of the voltage at the tank circuit to the reactance. The fractional change in frequency is 5×10^{-4} corresponding to a variation of the circuit inductance of 1×10^{-3}. For $Z_0=10\ \Omega$ this corresponds to $10^{-2}\ \Omega$ in good qualitative agreement with the computed reactance for the junction. As predicted by Eq. (21) the inductance is sensitive to variations in I_0 and insensitive to I_s.

A further observation of the nature of the junction was obtained with this capacitive coupling. The change in rf voltage as I_0 varies from a maximum to zero is antisymmetric about the center frequency of the circuit at $I_{0\max}$ with essentially no voltage on resonance. This demonstrates the purely dispersive nature of the junction at 30 Mc/sec.

CONCLUSION

We have quantitatively verified the dynamical behavior of Josephson junctions and compared this with the predictions of Josephson's equation. The Josephson junction behaves as a parametric inductance element in which the voltage is proportional to the frequency. When driven with a harmonic current source, the maximum voltage across the junction is the quantum voltage, $\hbar\omega/2e$. The current produces a rotation of the relative phase drop across the junction and the voltage results from the rate of change of the phase.

Through a measurement of the rf voltage as a function of magnetic flux we have measured the average phase drop across the junction and observed the diffraction effect in the coherent state. Thus the Josephson junction is a superconducting device which can be used completely in the superconducting state. The experiment reported here is in effect a demonstration of a parametric amplifier; the infinitesimal voltage applied to the junction by varying the flux over some time interval τ, $(\hbar/2e\tau)$, resulted in a change in the 30 Mc/sec "pump" voltage equal to $h\nu/2e$. Hence we have realized a voltage gain of $\nu\tau$; or for harmonic variation of the flux at a frequency ν_1 we would have a voltage gain to (ν/ν_1).